BIOCHEMISTRY
including biophysical chemistry & molecular biology

ARTICLE

pubs.acs.org/biochemistry

# Hypoxanthine Guanine Phosphoribosyltransferase Distorts the Purine Ring of Nucleotide Substrates and Perturbs the p$K_a$ of Bound Xanthosine Monophosphate

Spriha Gogia,[†] Hemalatha Balaram,[‡] and Mrinalini Puranik*[,†]

[†]National Centre for Biological Sciences, TIFR, GKVK Campus, Bellary Road, Bangalore 560065, India

[‡]Jawaharlal Nehru Centre for Advanced Scientific Research, Jakkur, Bangalore 560064, India

Supporting Information

**ABSTRACT:** Enzymatic efficiency and structural discrimination of substrates from nonsubstrate analogues are attributed to the precise assembly of binding pockets. Many enzymes have the additional remarkable ability to recognize several substrates. These apparently paradoxical attributes are ascribed to the structural plasticity of proteins. A partially defined active site acquires complementarity upon encountering the substrate and completing the assembly. Human hypoxanthine guanine phosphoribosyltransferase (hHGPRT) catalyzes the phosphoribosylation of guanine and hypoxanthine, while the *Plasmodium falciparum* HGPRT (PfHGPRT) acts on xanthine as well. Reasons for the observed differences in substrate specificities of the two proteins are not clear. We used ultraviolet resonance Raman spectroscopy to study the complexes of HGPRT with products (IMP, GMP, and XMP), in both organisms, in resonance with the purine nucleobase electronic absorption. This led to selective enhancement of vibrations of the purine ring over those of the sugar−phosphate backbone and protein. Spectra of bound nucleotides show that HGPRT distorts the structure of the nucleotides. The distorted structure resembles that of the deprotonated nucleotide. We find that the two proteins assemble similar active sites for their common substrates. While hHGPRT does not bind XMP, PfHGPRT perturbs the p$K_a$ of bound XMP. The results were compared with the mutant form of hHGPRT that catalyzed xanthine but failed to perturb the p$K_a$ of XMP.

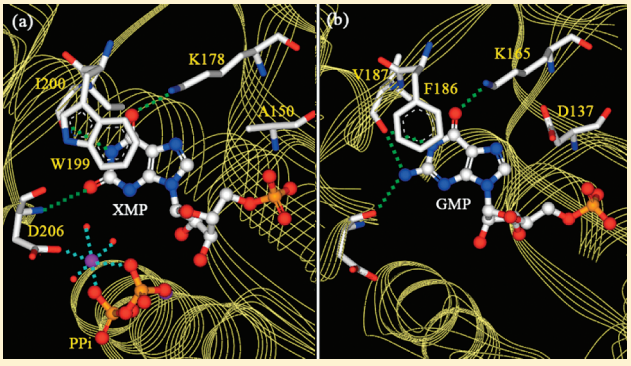


Understanding of physical interactions that lead to molecular recognition of substrates is central to understanding and manipulating enzyme function and to the rational design of inhibitors. X-ray and NMR spectroscopies are invaluable in providing information about these interactions in the form of three-dimensional structures. If structures of the enzyme−substrate (or substrate analogue) complex are available, the juxtaposition of substrates vis-à-vis the amino acids of the active site assists in deciphering the chemistry that takes place in the enzyme. However, if an enzyme displays substrate promiscuity or multiple-substrate specificity, structures of several enzyme−substrate complexes must be determined to understand the active site interactions and chemical mechanism in each case. Similarly, when apparently structurally analogous enzymes exhibit differing substrate specificities, high-resolution X-ray or NMR structures of each analogue with its substrate are needed to provide insight into the mechanisms of molecular recognition. Vibrational spectroscopy is a relatively underutilized tool that can provide detailed information about small molecule−protein interactions with selectivity and specificity even if only low-resolution structures are available from other techniques.

The vibrational Raman spectrum of a molecule is a chemical fingerprint that provides its unique identity. When this spectrum is obtained with an exciting line in resonance with the absorption of a specific ligand or substrate, it selectively yields the spectrum of that molecule even in the presence of a binding partner such as the enzyme. Importantly, interactions of the substrate with the active site of the enzyme result in perturbations in the band positions of the substrates. Thus, high-resolution Raman spectra of enzyme-bound substrates are a direct measure of the distortion of the substrate structure by the enzyme. In turn, the extent and direction of distortion of the substrate inform on the nature of the active site. In this work, we demonstrate the ability of Raman spectroscopy to detect subtle distortions in the purine base of the nucleotide when present within the active site of the enzyme hypoxanthine guanine phosphoribosyltransferase (HGPRT).

HGPRT converts free purine nucleobases to nucleotides and is a part of the salvage pathway in humans and other organisms. Parasitic protozoa like *Plasmodium falciparum* rely exclusively on nucleotides recycled through the salvage pathway. As a consequence, it has long been postulated that the enzyme is a potential

**Received:** December 22, 2010
**Revised:** April 11, 2011
**Published:** April 12, 2011

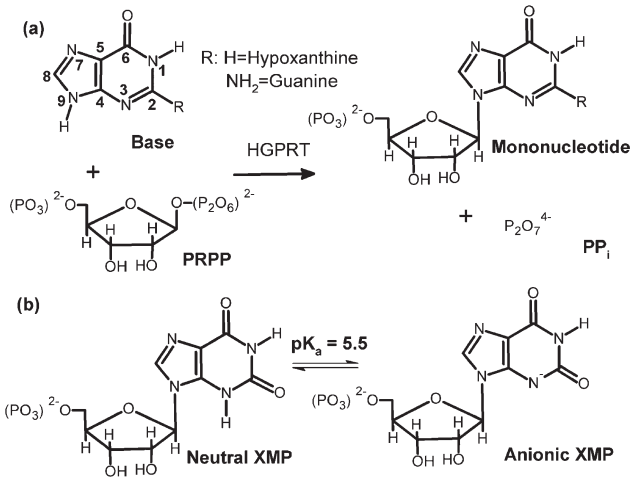


**Figure 1.** (a) Reaction catalyzed by human HGPRT. *P. falciparum* HGPRT catalyzes the conversion of xanthine to XMP in addition. (b) Structures of neutral and anionic XMP.

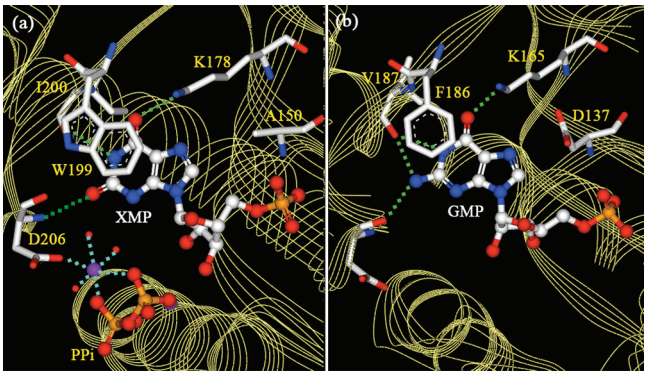


**Figure 2.** Active site of (a) *Toxoplasma gondii* HGPRT bound to XMP, pyrophosphate, and $Mg^{2+}$ (Protein Data Bank entry 1QKS) and (b) human HGPRT bound to GMP (Protein Data Bank entry 1HMP). Dashed green lines represent inferred hydrogen bonds between the purine ring of nucleotides and protein amino acids. Dashed cyan lines represent the coordinate bonds formed by one of the $Mg^{2+}$ ions (purple). Aromatic residues [(a) W199 and (b) F186] form a $\pi$-stack atop the pyrimidine ring.

therapeutic target for the development of antiparasitic drugs.[1−3] Both human HGPRT (hHGPRT) and *P. falciparum* HGPRT (PfHGPRT) convert hypoxanthine and guanine into inosine monophosphate (IMP) and guanosine monophosphate (GMP), respectively, in an $Mg^{2+}$-dependent reaction. The ribose phosphate from phosphoribosyl pyrophosphate (PRPP) (Figure 1a) is transferred to the N9 atom of the free purine base. While the activity of PfHGPRT for hypoxanthine and guanine is lower than that of the human enzyme,[4] remarkably, it is able to phosphoribosylate xanthine[1,5] and many more non-natural nucleobases.[6] Table S1 of the Supporting Information summarizes the measured kinetic parameters and the dissociation constants for the three natural substrates of HGPRTs investigated in this work.

Overall, structures of the various HGPRTs are highly similar (44% identical sequences for human and *P. falciparum*),[7] containing a conserved PRPP motif and a flexible loop that covers and sequesters the active site from the solvent during catalysis.[8] While several crystal structures of the human enzyme bound to different ligands are available,[8−12] only a single structure of the PfHGPRT bound to a transition-state analogue is known.[13] An enduring puzzle is how the oxo group of xanthine is accommodated at the same site that forms contacts with the exocyclic $NH_2$ group of guanine in the parasite enzyme given the reversed requirement of hydrogen bonding partners (Figure 2). The presence of crystal water, which could potentially explain this conundrum, is not found at this site in the available crystal structure of hHGPRT bound to IMP.[11] This also raises the question of whether the two HGPRTs recognize their common substrates through similar interactions.

In the following, with extensive experiments with hHGPRT, we first demonstrate that Raman spectra of bound nucleotides are indeed highly informative with respect to the active site interactions. Further, we show that despite their differences, enzymes from the two organisms modulate the nucleotide geometries to assemble precisely the same active site configurations for their common products. We then extend the investigation to XMP that binds only PfHGPRT. Our data reveal that the active site of PfHGPRT perturbs the $pK_a$ of bound XMP. While XMP in solution at pH 7.0 is in the anionic form (Figure 1b),[14] XMP bound to PfHGPRT exists as a mixture of the neutral and anionic forms at the same pH. We also used an interesting, non-active site mutation in the human enzyme (F36L) that catalyzes xanthine,[4] to compare the human and *Plasmodium* enzymes. We show that although the F36L mutation expands the substrate specificity of hHGPRT, the active site assembled in the modified human enzyme is unable to achieve the same structural configuration as that in PfHGPRT. This is a first report that describes the subtle changes in the electronic characteristics of IMP, GMP, and XMP when bound to HGPRT.

## MATERIALS AND METHODS

**Enzyme Purification and Assay.** *Escherichia coli* strain BL21-(DE3) transformed with pET23d containing the human HGPRT gene was used for protein expression. The enzyme was purified as reported previously[7] using a Q-Sepharose (GE Healthcare) column for anion exchange instead of a ResQ column. PfHGPRT was overexpressed in *E. coli* strain S$\varphi$609 transformed with the expression construct in vector pTrc99A and purified as described previously.[15]

Protein concentrations were determined by using the method of Bradford, using 1 mg/mL BSA as a standard. An activity assay, as described previously,[15] was conducted after each new batch of protein purification to ascertain that the enzyme was active. The activity was found to be unaffected in the presence of 30 mM sodium nitrate, used as internal standard in Raman experiments.

**Sample Preparation for End Product Binding Experiments.** IMP, GMP, XMP, sodium nitrate, and $MgCl_2$ were obtained from Sigma Co. Nucleotide stocks (10 mM) were prepared in water and diluted to 450 $\mu$M in 20 mM Tris-HCl (pH 7.0) for experiments with the human enzyme and in 20 mM potassium phosphate (pH 7.0) for experiments with the *P. falciparum* enzyme. Purified human HGPRT was stored in 20 mM Tris-HCl (pH 7.0), 10% glycerol, and 1 mM dithiothreitol (DTT). The human enzyme was incubated at 4 °C after the DTT concentration had been increased to 5 mM overnight before Raman experiments were conducted. Purified *P. falciparum* HGPRT was stored in 20 mM potassium phosphate (pH 7.0), 20% glycerol, and 2 mM DTT. This enzyme was incubated with 60 $\mu$M IMP and 5 mM DTT 3 h before the experiment was conducted. For experiments at pH 8.5, the storage buffer of

PfHGPRT was changed to 20 mM potassium phosphate (pH 8.5), 20% glycerol, and 2 mM DTT by dialysis.

For the H−D exchange experiments, buffers were prepared in $D_2O$. Human HGPRT was exchanged with 20 mM Tris-HCl, 10% glycerol, and 1 mM DTT prepared in $D_2O$ by employing an Amicon Ultra Centrifugal filter (Millipore). Similarly, PfHGPRT was exchanged with 20 mM potassium phosphate (pH 7.0), 20% glycerol, and 2 mM DTT prepared in $D_2O$. Nucleotide (GMP, IMP, and XMP) stocks were prepared by dissolving the required amount in $D_2O$.

The nucleotide binding experiments involved recording the resonance Raman spectra using excitation at 260 nm of three types of solutions: (a) hHGPRT/PfHGPRT (150 $\mu$M) and 12 mM $MgCl_2$ with 30 mM sodium nitrate, (b) hHGPRT/PfHGPRT (150 $\mu$M), IMP/GMP/XMP (450 $\mu$m), and 12 mM $MgCl_2$ with 30 mM sodium nitrate, and (c) 450 $\mu$M IMP/GMP/XMP (pH 7.0) with 30 mM sodium nitrate. Spectra of all the buffers were recorded with an internal standard (30 mM sodium nitrate) to serve as reference spectra for subtraction.

**Ultraviolet Resonance Raman Spectroscopy.** The detailed UVRR setup has been described in a previous publication.[16] All experiments reported in this work were conducted with 260 nm Raman excitation that was generated by a Ti−S laser (Indigo, Coherent Inc.) pumped by the frequency-doubled output of a nanosecond-pulsed Nd:YLF laser (Evolution, Coherent Inc.) at 527 nm (1 kHz repetition rate). At the sample, average power was kept below ~600 $\mu$W. Light scattered from the sample was analyzed using a monochromator (Jobin-Yvon) equipped with a 3600 grooves/mm grating for dispersing the light. Spectra were recorded with a 1024 × 256 pixel, back-illuminated CCD camera (Jobin-Yvon) and calibrated using known solvent bands. The solvents used were dimethylformamide, cyclohexane, acetonitrile, trichloroethylene, 2-propanol, and indene (HPLC grade from Ranchem chemicals and Sigma Co.) and were used without further purification.

In experiments where the relative shift was measured, the spectra were recorded without changing the spectrometer position and intense bands are accurate to ±1 $cm^{-1}$. All spectral processing was conducted using SynerJY (Jobin-Yvon). Band positions were determined by fitting Lorentzian line shapes to the bands in the observed spectra. Although we have previously characterized the spectra of the nucleotides,[17] the spectrum of each nucleotide was recorded on each experiment day just before or after the spectrum of the enzyme·nucleotide sample had been recorded to minimize errors due to grating movement.

UVRR spectra of nucleotides bound to HGPRT were obtained by taking a 1:3 HGPRT:nucleotide ratio, in the presence of $Mg^{2+}$ ions, to achieve maximal binding of the nucleotide to the enzyme. The spectrum of the unbound nucleotide was subtracted from that of the HGPRT·nucleotide mixture. All samples contained 30 mM sodium nitrate as described above. The Raman band of nitrate at 1048 $cm^{-1}$ was used as an internal standard for normalization of intensities across spectra. Similar UVRR experiments were also conducted with the hHGPRT·AMP mixture [adenosine monophosphate (see Figure S1 in the Supporting Information)] to serve as a check for the presence of nonspecific binding. Because AMP does not bind to hHGPRT,[18] no shifted peaks were obtained for this molecule in the presence of hHGPRT. Spectra were recorded at 260 nm excitation by typically averaging 40 frames of 40 s exposure each. It was ensured that there was no sample damage via comparison of the first and last frame (40th) of the data. The change in the Raman shifts ($\Delta\Delta\nu$), for each vibrational band listed in the tables, is the mean shift obtained by averaging over data from several independent experiments conducted on different days. Larger errors are usually obtained for bands with weak intensity because of uncertainty in the fitting of the band shapes.

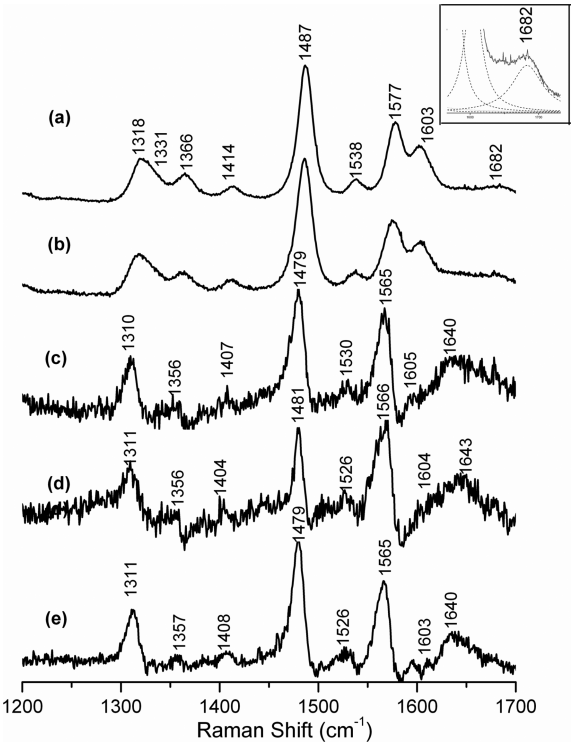


**Figure 3.** UVRR spectra of (a) GMP at pH 7 (inset shows an enlarged view, and Lorentzian fit to the 1682 $cm^{-1}$ band of GMP assigned to the carbonyl stretching mode), (b) [hHGPRT·GMP+free GMP+free hHGPRT] minus free hHGPRT, (c) hHGPRT·GMP (b−a), (d) PfHGPRT·GMP, and (e) F36L hHGPRT·GMP. The GMP concentration was 450 $\mu$M, and the HGPRT concentration was 150 $\mu$M.

## RESULTS

The stable state probed in the following spectroscopic experiments in which the Raman signal is acquired over several minutes is the nucleotide·HGPRT complex. The forward reaction of the enzyme is fast ($k_{cat}$ values of 6 $s^{-1}$ for hypoxanthine substrate and 13 $s^{-1}$ for guanine substrate), and the rate-limiting step is the dissociation of the nucleotide product from the enzyme following the release of $PP_i$.[11]

We exploited the different electronic absorption spectra of proteins and nucleic acids by using a Raman excitation wavelength in resonance with purine nucleobases at 260 nm. This results in exclusive enhancement of vibrational bands from the nucleobase without interference from either the sugar−phosphate backbone of the nucleotide or the protein in the nucleotide−protein complex as seen in Figure 3c. The small spectral contribution from protein at this wavelength (Figure S2 of the Supporting Information) was removed by subtraction.

**The Active Site of hHGPRT Distorts the Guanine Nucleobase of Bound GMP To Weaken the N1−H and C=O Bonds.** The UVRR spectra of GMP in buffer and the hHGPRT·GMP complex in resonance with the nucleobase are shown in Figure 3 (a and c, respectively). The spectrum of the complex contains intense bands at 1640, 1565, 1479, 1407, and 1310 $cm^{-1}$. A detailed normal-mode analysis of GMP has been reported previously.[17] The corresponding bands of unperturbed GMP occur at 1682, 1577, 1487, 1414, and 1318 $cm^{-1}$, respectively (a typical downshift of 7−11 $cm^{-1}$ barring the carbonyl mode).

**Table 1. Comparison of Shifts in Wavenumber Observed in UVRR Spectra of hHGPRT·GMP, F36L hHGPRT·GMP, and PfHGPRT·GMP Complexes with Respect to GMP in Buffer at pH 7 and Shifts Observed with Deuterium Labeling of GMP and the hHGPRT·GMP Complex ($\nu_{D_2O}$ minus $\nu_{H_2O}$)**

| | GMP | | | hHGPRT·GMP[b] | F36L hHGPRT·GMP[b] | PfHGPRT·GMP[b] | hHGPRT·GMP | |
|---|---|---|---|---|---|---|---|---|
| composition[a] | $H_2O$ | $D_2O$ | shift in $D_2O$[c] | $H_2O$ | $H_2O$ | $H_2O$ | $D_2O$ | shift in $D_2O$[c] |
| St C6O+Be N1H | 1682 | 1665 | −19 | 1640 (−40) | 1640 (−42) | 1643 (−40) | 1648/1614 | 8/−26 |
| Py ring+Sci NH2+Be N1H | 1603 | 1572 | −31 | 1605 (2) | 1603 (2) | 1604 (2) | 1574 | −30 |
| Sci NH2+Py ring+Be N1H | 1577 | 1582 | 5 | 1565 (−11) | 1565 (−10) | 1566 (−12) | 1568 | 3 |
| Pu ring+Be N1H+C8H+Sci NH2 | 1538 | 1540 | 2 | 1530 (−11) | 1526 (−10) | 1526 (−10) | 1532 | 2 |
| St N7C8+Py ring+Be C8H +N1H+N2H2b | 1487 | 1480 | −7 | 1479 (−7) | 1479 (−7) | 1481 (−7) | 1470 | −9 |
| Py ring+St N7C8+rock NH2+Be N1H | 1414 | 1405 | −9 | 1407 (−7) | 1408 (−7) | 1404 (−7) | 1398 | −9 |
| Pu ring+Be N2H2a | 1366 | 1355 | −11 | 1356 (−8) | 1357 (−7) | 1356 (−9) | 1348 | −6 |
| Be N1H+N2H2b+C8H +St C5N7−C2N2 | 1318 | 1318 | 0 | 1310 (−8) | 1311 (−8) | 1311 (−7) | 1314 | 4 |

[a] Abbreviations: St, stretch; Be, bend; Py, pyrimidine; Sci, scissors; Pu, purine. [b] Values in parentheses are average shifts ($\nu_{HGPRT\cdot GMP}$ minus $\nu_{GMP}$) obtained from three or more data sets. [c] Shifts correspond to the shifts in wavenumber obtained upon going from $H_2O$ to $D_2O$ ($\nu_{D_2O}$ minus $\nu_{H_2O}$).

These shifts are summarized in Table 1 along with the primary mode composition of each of these bands. Formation of the hHGPRT·GMP complex causes changes not only in the positions but also in the relative intensities of the bands.

The carbonyl stretching mode of GMP undergoes a large downshift of 40 $cm^{-1}$ when GMP binds to hHGPRT. This is in accordance with the interaction of the C═O group of GMP with Lys165 in the active site via hydrogen bonding observed in the X-ray crystal structure. In free GMP, this mode is known to undergo an H−D isotopic shift of 19 $cm^{-1}$ in $D_2O$ due to contributions from N1−H bending motion.[16] The large downshift observed in the enzyme complex reflects interactions of the N1−H and C═O groups with the protein side chains. Further support for hydrogen bonds at both the N1−H group and O6 is provided by a comparison with the GMP anion. The GMP anion is formed via deprotonation of the hydrogen at N1. This leads to a downshift in the observed wavenumber of the carbonyl mode to 1592 $cm^{-1}$ ($\Delta\nu$ = 90 $cm^{-1}$).[17] The position of the carbonyl stretching mode of the hHGPRT·GMP complex is intermediate between that of the neutral and anionic forms of free GMP. The hydrogen bond between Lys165 and the carbonyl group of GMP is proposed to confer specificity for 6-oxopurine binding at the enzyme active site.[19] Observed Raman shifts indicate that this interaction leads to an increase in the C═O bond length. The large downshift observed in this mode is also partly attributed to hydrogen bonding interactions of the N1−H bond of the purine ring of GMP with the backbone carbonyl of Val187 in the active site of the enzyme. Similar downshifts in the carbonyl mode, attributed to hydrogen bonds, have been observed in the uracil−uracil DNA glycosylase complex by Dong et al.[20] and in the 4-hydroxycinnamyl chromophore in the photoactive yellow protein (PYP) by Unno et al.[21]

The pyrimidine stretching mode of GMP coupled to $NH_2$ scissoring observed at 1577 $cm^{-1}$ in GMP downshifts by 11 $cm^{-1}$ in the hHGPRT·GMP complex. This downshift can be attributed to hydrogen bonds formed with the $NH_2$ group at the active site. The band at 1487 $cm^{-1}$, arising from Im N7−C8 stretching and the pyrimidine ring and the N1−H bend, is downshifted by 7 $cm^{-1}$. Coincidentally, a similar magnitude of downshift is observed in this band upon H−D exchange in GMP.[17] Although the close match is fortuitous, the observed downshift in both cases indicates that N1−H group is involved in hydrogen bonding with residues of the active site. The difference in the magnitude of the shifts (11 and 7 $cm^{-1}$) of the two bands discussed above is consistent with the descriptions of their modes. While two hydrogen bonds influence the 1577 $cm^{-1}$ mode, only one participating atom is affected in the mode at 1487 $cm^{-1}$. The two lower-intensity bands at 1407 $cm^{-1}$ ($\Delta\nu$= −7) and 1310 $cm^{-1}$ ($\Delta\nu$ = −8) correspond to modes that are comprised of N1−H and $NH_2$ motions and reinforce the presence of hydrogen bonding interactions at the active site of hHGPRT.

These data indicate that the active site contacts observed in the X-ray structure are largely preserved in solution for HGPRT. The N1, C6═O, and exocyclic $NH_2$ groups of the guanine base participate in hydrogen bonding with active site residues Val187, Asp193, and Lys165 (Figure 2b), leading to the perturbations in the Raman spectrum discussed above.

Relative intensities of the GMP bands are also altered in the active site pocket. While the intensity of the 1605 and 1479 $cm^{-1}$ modes is suppressed, that of the band at 1565 $cm^{-1}$ is enhanced (Figure 3c). Phe186 is positioned to form a $\pi$ stack with the pyrimidine ring in the crystal structure (Figure 2b). The observed intensity changes in the Raman spectra confirm this interaction. We simulated the effect of Phe stacking on the Raman intensities of GMP using DFT calculations. A depression in the intensities of the obtained Raman bands is predicted as a result of aromatic $\pi$ stacking from these calculations, which can be seen in Table S2 of the Supporting Information.

Comparison of the spectrum of the hHGPRT·GMP complex with that of GMP anion yields similarities with respect to the relative intensity ratios in the wavenumber region from 1400 to 1600 $cm^{-1}$, especially the loss of intensity of the band at 1605 $cm^{-1}$. While the wavenumbers of the bands in the spectrum of the hHGPRT·GMP complex are intermediate between those of free GMP and deprotonated GMP, the intensity ratios correspond to those of anionic GMP. On the basis of these observations, we conclude that upon binding to the enzyme, the structure of the guanine nucleobase of the bound GMP is distorted from that in neutral form to one that resembles the GMP anion. Raman spectra thus provide unprecedented, detailed information about the electronic structure of the ligand.

**Isotope-Edited Spectra of the hHGPRT·GMP Complex.** Comparison of the isotope-induced shifts observed in the


dx.doi.org/10.1021/bi102039b |*Biochemistry* 2011, 50, 4184–4193

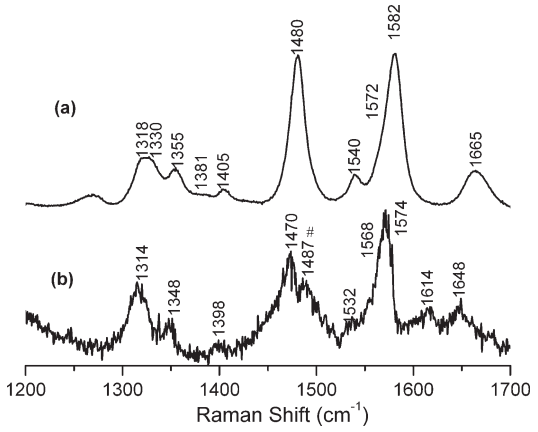


**Figure 4.** UVRR spectra of (a) GMP in $D_2O$ at pD 7 and (b) the hHGPRT·GMP complex in $D_2O$. The number sign denotes the band from unexchanged GMP. The GMP concentration was 450 $\mu$M, and the HGPRT concentration was 150 $\mu$M.

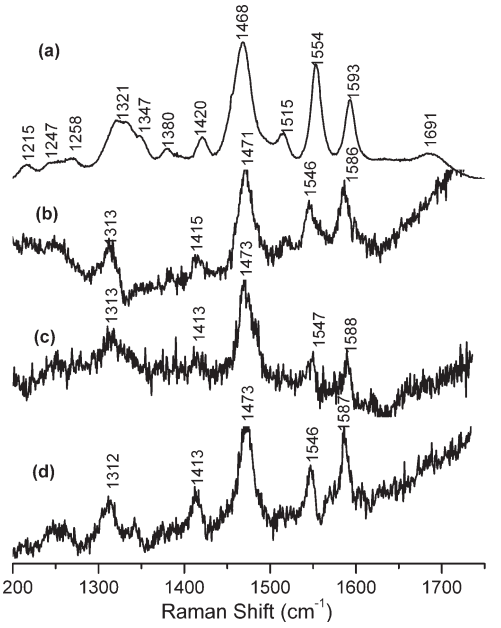


**Figure 5.** UVRR spectra of (a) IMP at pH 7, (b) the hHGPRT·IMP complex, (c) the PfHGPRT·IMP complex, and (d) the F36L hHGPRT·IMP complex. The IMP concentration was 450 $\mu$M, and the HGPRT concentration was 150 $\mu$M.

hHGPRT·GMP complex with those in free GMP would help identify alterations, if any, in the composition of normal modes of GMP upon binding to the enzyme. Figure 4a displays the spectrum of neutral GMP in $D_2O$.[16] The enzyme-bound GMP undergoes isotope-induced shifts in all observed bands: 1574 $cm^{-1}$ [$\Delta\nu_{(H\ to\ D)} = -30$], 1568 $cm^{-1}$ [$\Delta\nu_{(H\ to\ D)} = 3$], 1470 $cm^{-1}$ [$\Delta\nu_{(H\ to\ D)} = -9$], 1348 $cm^{-1}$ [$\Delta\nu_{(H\ to\ D)} = -6$], and 1314 $cm^{-1}$ [$\Delta\nu_{(H\ to\ D)} = 4$] (Figure 4b and Table 1). The isotopic shifts of the hHGPRT·GMP complex correlate very well with those observed upon H−D exchange in free GMP[16] (Table 1), indicating that the normal mode description remains largely unchanged despite interactions with the active site. These shifts also confirm that all the protons of the nucleobase are still bound to it in the active site. We observe that the C6═O mode has two components in $D_2O$. This band is weak, and a corresponding split in the $H_2O$ spectrum cannot be ruled out. This may be due to the presence of two slightly different orientations of the Lys that make hydrogen bonding contacts with the C═O group.

**Interactions of IMP with the Active Site.** The spectrum of IMP bound to human HGPRT (Figure 5b) shows that the bands corresponding to the nucleobase vibrations shift with respect to those in neutral IMP. The bands at 1586 $cm^{-1}$ ($\Delta\nu = -7$), 1546 $cm^{-1}$ ($\Delta\nu = -9$), 1471 $cm^{-1}$ ($\Delta\nu = 4$), 1415 $cm^{-1}$ ($\Delta\nu = -6$), and 1313 $cm^{-1}$ ($\Delta\nu = -10$) are shifted by the amounts indicated in parentheses (Table 2). While most modes display a downshift with respect to free IMP analogous to the case of the hHGPRT·GMP complex, the band at 1471 $cm^{-1}$ is upshifted by 4 ± 2 $cm^{-1}$.

The normal mode corresponding to the band at 1593 $cm^{-1}$ comprises the pyrimidine ring coupled to C2−H and N1−H bending. The downshift in this band in the hHGPRT·IMP complex to 1586 $cm^{-1}$ indicates an interaction of the N1 proton of IMP with the active site.

The N3C4−C4C5−N7C8 stretching vibration downshifts from 1554 $cm^{-1}$ in aqueous IMP to 1549 $cm^{-1}$ in $D_2O$. The corresponding band in the hHGPRT·IMP complex (1546 $cm^{-1}$) displays a similar downshift with respect to aqueous IMP.

The most intense band in the IMP spectrum (1468 $cm^{-1}$) appears at 1471 $cm^{-1}$ in the protein-bound spectrum. Similar to the upshift observed upon binding to the protein, when free IMP is deprotonated, this band upshifts from 1468 $cm^{-1}$ (pH 7) to 1473 $cm^{-1}$ (pH 11).[17] These shifts confirm that the hydrogen bonding interactions observed in the crystal structure are retained in solution and that contact with amino acids of the active site apparently restrains the N1−H bending vibration. The overall trend of downshifts in 6−10 wavenumbers indicates that the structure of IMP in the active site is perturbed from that of neutral IMP in solution to that of deprotonated IMP in which the N1 proton is absent.

**Active Sites of PfHGPRT and hHGPRT Provide Similar Environments for IMP and GMP.** The active sites of the two enzymes have a degree of sequence homology as high as 80%.[22] While a host of crystal structures are available for hHGPRT,[8−10,12] only a single crystal structure of the *Plasmodium* enzyme is available.[13] This cocrystal structure with the transition-state analogue, immucillinHP, shows an active site similar to that of hHGPRT, so that the reason for the observed differing substrate specificity in the two enzymes is not clear.

In the preceding section, we showed that the UVRR spectra of hHGPRT·GMP and hHGPRT·IMP complexes prove to be highly sensitive to the active site environment. Because these experiments correspond to solution structures, we expect that the UVRR spectra will be able to detect differences in the hydrogen bonding interactions of IMP and GMP in the two enzymes. Spectra of the complexes of PfHGPRT with GMP (PfHGPRT·GMP) and IMP (PfHGPRT·IMP) are shown in Figures 3d and 5c, respectively. A comparison with the corresponding spectra of hHGPRT (Figures 3c and 5b, respectively) shows that the perturbations introduced into the spectra upon binding of enzyme to the nucleotide are equivalent in the two enzymes. The fact that these shifts are comparable not only for IMP but also for GMP (Tables 1 and 2) indicates that the quantitative agreement in Raman shifts is not fortuitous. Despite their differences, hHGPRT and PfHGPRT achieve highly similar active site configurations. Additional support for these interactions

**Table 2. Comparison of Shifts in Wavenumber Observed in UVRR Spectra of hHGPRT·IMP, F36L hHGPRT·IMP, and PfHGPRT·IMP Complexes with Respect to IMP in Buffer at pH 7 and Wavenumber Shifts Observed upon Deuterium Labeling of IMP and the PfHGPRT·IMP Complex**

| | IMP | IMP[b] | IMP | hHGPRT·IMP[c] | F36L hHGPRT·IMP[c] | PfHGPRT·IMP[c] | PfHGPRT·IMP |
|---|---|---|---|---|---|---|---|
| composition[a] | $H_2O$ | $D_2O$ | shift in $D_2O$[d] | $H_2O$ | $H_2O$ | $H_2O$ | shift in $D_2O$[d] |
| Py ring+Be C2H+N1H | 1593 | 1580 | −13 | 1586 (−7) | 1587 (−8) | 1588 (−7) | −11 |
| St N3C4−C4C5−N7C8+Be C8H | 1554 | 1549 | −5 | 1546 (−9) | 1546 (−9) | 1547 (−8) | −3 |
| Be N1H+C8H+Pu ring | 1468 | 1428 | −40 | 1471 (4) | 1473 (4) | 1473 (4) | −52 |
| Be N1H+C2H+Py ring | 1420 | 1334 | −86 | 1415 (−6) | 1413 (−7) | 1413 (−7) | −78 |
| Be C8H+C2H+N1H+Pu ring | 1321 | 1309 | −11 | 1313 (−10) | 1312 (−10) | 1313 (−8) | −8 |

[a] Abbreviations: St, stretch; Be, bend; Py, pyrimidine; Pu, purine. [b] Taken from ref 17. [c] Values in parentheses are average shifts ($\nu_{HGPRT\cdot IMP}$ minus $\nu_{IMP}$) obtained from three or more data sets. [d] Shifts correspond to the shifts in wavenumber obtained upon going from $H_2O$ to $D_2O$ ($\nu_{D_2O}$ minus $\nu_{H_2O}$).

is provided by H−D exchange-induced shifts in the IMP complex of the enzyme in $D_2O$ (Table 2).

The crystal structure of IMP in a complex with human HGPRT has been determined by Xu et al.[11] This structure was found to be isomorphous with the hHGPRT·GMP structure, and similar hydrogen bonding contacts were predicted for the purine binding site with the exception of the contacts with the $NH_2$ group of GMP. In accordance with these data, we find that most modes of IMP and GMP, barring the carbonyl mode, are perturbed by 7−11 wavenumbers in the HGPRT active sites, indicating similar distortions in both molecules.

**The p$K_a$ of XMP Is Perturbed When It Binds to PfHGPRT.** The spectrum of XMP bound to PfHGPRT at pH 7.0 is shown in Figure 6c. A large number of bands that are perturbed from their corresponding positions in aqueous XMP (pH 7) are observed. Like the spectra of HGPRT·IMP and HGPRT·GMP complexes, this spectrum shows systematic downshifts with respect to the spectrum of aqueous XMP (pH 7). In addition, the spectrum also displays altered relative intensities of the Raman bands. Poorer binding of XMP to PfHGPRT ($K_m$ for xanthine of 261 ± 52 $\mu$M compared to values of <1 $\mu$M for hypoxanthine and guanine[4]) compared to that of IMP and GMP is reflected in the lower signal-to-noise ratio of this spectrum. As anticipated, no change in the Raman bands of XMP is observed when it is mixed with wild-type hHGPRT, indicating that binding does not take place (Figure S3a of the Supporting Information).

XMP is unique among 6-oxopurine nucleotides because it exists as an anion at pH 7.0 (p$K_a$ = 5.5)[14] while others are in their neutral forms (Figure 1b). The first deprotonation occurs at N3, which leaves the N1−H proton intact and available to make active site contacts similar to those made by the N1−H group in IMP and GMP.[14,17] The UVRR spectrum of aqueous XMP obtained with 260 nm excitation at pH 7.0 is shown in Figure 6f and has been previously assigned to its anion.[17] The same work also reported detailed assignments of the bands of $XMP^-$ and neutral XMP in water and $D_2O$.[17] In the following interpretation of the UVRR spectra of the PfHGPRT·XMP complex, we refer to the normal mode descriptions reported therein.

The band at 1654 $cm^{-1}$ in the PfHGPRT·XMP complex arises from the carbonyl bond stretching vibration. This mode is observed at 1651 $cm^{-1}$ in $XMP^-$ and at 1696 $cm^{-1}$ in neutral XMP.[17] Thus, the C=O bond length in the enzyme-bound XMP structure is closer to its bond length in $XMP^-$. The most intense band in the spectrum of aqueous $XMP^-$ at 1573 $cm^{-1}$ arises from pyrimidine ring stretching and C8−H bending. In the spectrum of the PfHGPRT·XMP complex, this mode is observed

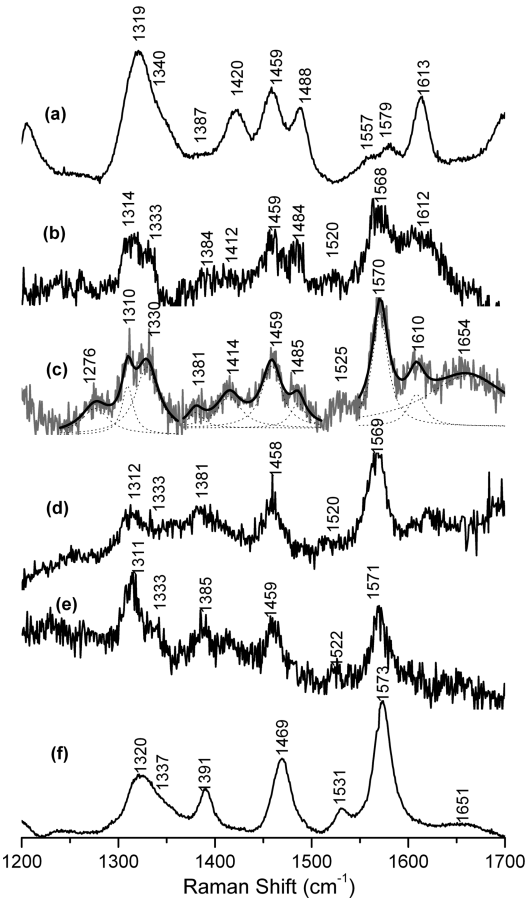


**Figure 6.** UVRR spectra of (a) XMP at pH 2, (b) the PfHGPRT·XMP complex at pH 6.5, (c) the PfHGPRT·XMP complex at pH 7.0 (dotted lines depict Lorentzian fits made to the obtained spectrum), (d) the PfHGPRT·XMP complex at pH 8.5, (e) the F36L hHGPRT·XMP complex at pH 7.0, and (f) XMP at pH 7. The XMP concentration was 450 $\mu$M, and the HGPRT concentration was 150 $\mu$M.

at 1570 $cm^{-1}$. The corresponding band is at a higher wavenumber (1613 $cm^{-1}$) in neutral XMP (Figure 6a).[17]

The 1525 $cm^{-1}$ band in the PfHGPRT·XMP complex corresponds to the 1531 $cm^{-1}$ band of $XMP^-$. These bands are attributed to C8−H bending vibrations with a slight contribution from the imidazole ring as well. The 6 $cm^{-1}$ downshift in this mode indicates that the C8−H vibration is

**Table 3. Comparison of Shifts in Wavenumber Observed in UVRR Spectra of the F36L hHGPRT·XMP and PfHGPRT·XMP Complexes with Respect to XMP in Buffer at pH 7 and 2 and Wavenumber Shifts Observed upon Deuterium Labeling of XMP (at pH 2 and 7) and the PfHGPRT·XMP Complex**

| | XMP neutral | | XMP anion | | F36L hHGPRT·XMP[b] | PfHGPRT·XMP[b] | | PfHGPRT·XMP | |
|---|---|---|---|---|---|---|---|---|---|
| composition[a] | pH 2 | shift in $D_2O$[c] | pH 7 | shift in $D_2O$[c] | shift from pH 7, XMP | shift from pH 2, XMP | shift from pH 7, XMP | shift in $D_2O$[c] | |
| St C6═O+C2═O | 1696 | 2 | 1651 | −2 | | 1654 (−42) | 1654 (4) | 2 | anion |
| Py ring | 1613 | −6 | | | | 1610 (−2) | | −17 | neutral |
| Py ring+Be C8H | | | 1573 | 2 | 1571 (−2) | | 1570 (−4) | 0 | anion |
| Be C8H+St N7C8+C4N9 | | | 1531 | −3 | 1522 (−7) | | 1525 (−6) | 9 | anion |
| St N7C8+Be C8H+N3H | 1488 | −7 | | | | 1485 (−4) | | −5 | neutral |
| Be N3H+N1H+Im ring | 1459 | −26 | | | | | | | anion |
| Py ring+N7C8+Be C8H | | | 1469 | 0 | 1458 (−11) | | 1459 (−12) | −2 | |
| Be N1H+ Im ring+St N1C6 | 1420 | 2 | | | | 1414 (−7) | | | neutral |
| Be N1H+St C8N9+C4C5 | 1387 | −7 | 1391 | 0 | 1385 (−4) | 1381 (−7) | 1381 (−10) | 6 | neutral/anion |
| Be N1H+C8H+Pu ring | 1340 | −5 | 1337 | −4 | 1333 (−4) | 1330 (−10) | 1330 (−7) | −4 | neutral/anion |
| Be N1H+C8H+St N1C2 | 1319 | −8 | 1320 | −5 | 1311 (−9) | 1310 (−12) | 1310 (−12) | 5 | neutral/anion |

[a] Abbreviations: St, stretch; Be, bend; Py, pyrimidine; Pu, purine; Im, imidazole. [b] Values in parentheses are average shifts ($\nu_{HGPRT\cdot XMP}$ minus $\nu_{XMP}$) obtained from three or more data sets. [c] Shifts correspond to shifts in wavenumbers obtained upon going from $H_2O$ to $D_2O$ ($\nu_{D_2O}$ minus $\nu_{H_2O}$).

also influenced by enzyme binding. The pyrimidine ring mode at 1469 $cm^{-1}$ in $XMP^-$ shifts to 1459 $cm^{-1}$ in the PfHGPRT·XMP complex.

Other bands observed in the spectrum of the PfHGPRT·XMP complex cannot be attributed to the anionic form of XMP. From the intensity patterns and the positions, these are identified as bands of neutral XMP (Figure 6a). The band at 1610 $cm^{-1}$ in the PfHGPRT·XMP complex corresponds to the pyrimidine stretching mode observed at 1613 $cm^{-1}$ in neutral XMP. Bands at 1485 and 1414 $cm^{-1}$ correspond to bands in neutral XMP at 1488 and 1420 $cm^{-1}$, respectively. The primary contribution to the modes giving rise to these bands is from N7−C8 stretching and N1−H bending vibrations, respectively.

Lower-wavenumber bands corresponding to both species are observed as well. The bands at 1381, 1330, and 1310 $cm^{-1}$ in the spectrum of the PfHGPRT·XMP complex correspond to the 1391 and 1387 $cm^{-1}$, 1337 and 1340 $cm^{-1}$, and 1320 and 1319 $cm^{-1}$ bands from anionic and neutral XMP, respectively. Because these bands are downshifted from their positions in neutral and anionic XMP, an unequivocal assignment to specific species cannot be made for these bands (summarized in Table 3).

From the data described above, it is clear that many features in the spectrum of the PfHGPRT·XMP complex correspond to those in the spectrum of XMP at pH 2, including two bands around 1400 $cm^{-1}$ and the band at 1610 $cm^{-1}$ that is absent from the spectrum of anionic XMP. Several other bands in the spectrum of the PfHGPRT·XMP complex correspond to those in the spectrum of XMP at pH 7, e.g., the bands at 1570 and 1525 $cm^{-1}$. This suggests that XMP in the active site of PfHGPRT exists as a mixture of the neutral (N3−H) and anionic (deprotonated at N3) forms.

**PfHGPRT·XMP Complex in $D_2O$.** Using H−D exchange-induced isotopic Raman shifts, we find that binding to the protein does not significantly alter the normal mode composition for most modes of the XMP complex because deuterium-induced shifts are similar in magnitude to those of the substrate in water or $D_2O$ (Table 3 and Figure S4 of the Supporting Information). In the PfHGPRT·XMP complex, modes arising from both anionic and neutral forms that we observed in $H_2O$ are also seen in $D_2O$ at expected shifts, further confirming the presence of these two forms in the active site of PfHGPRT.

A few bands do show altered H−D exchange shifts and hence mode composition changes as listed in Table 3. The 1531 $cm^{-1}$ band of unbound $XMP^-$ downshifts by 3 $cm^{-1}$ in $D_2O$, while the band of the PfHGPRT·XMP complex shows an upshift of 9 $cm^{-1}$ upon deuterium labeling. Thus, there is a large change in the mode composition of this mode upon binding of PfHGPRT. On the basis of similar reasoning, it can be concluded that normal mode distributions of the 1391 and 1320 $cm^{-1}$ bands of $XMP^-$ are altered when this molecule is bound to PfHGPRT.

**Mutant hHGPRT with Expanded Substrate Specificity.** Although hHGPRT does not catalyze xanthine, a mutant of hHGPRT, F36L, does catalyze the conversion of xanthine to XMP[4] with a $k_{cat}$ much lower than those of hypoxanthine and guanine. F36 is present at the base of loop IV that is involved in purine recognition. It was suggested that this mutation rearranges the active site such that the repulsive interactions with the C2═O group of XMP and xanthine are avoided. To probe if the rearranged active site in this mutant form of hHGPRT is similar to that of PfHGPRT, we probed complexes of F36L hHGPRT with the three products, IMP, GMP, and XMP.

**The Active Site Environment of IMP and GMP in F36L hHGPRT Is Similar to That in Wild-Type hHGPRT.** We first studied binding of the end products, IMP and GMP, to F36L hHGPRT for comparison with the active site of the wild-type enzyme. The UVRR spectra of GMP bound to F36L hHGPRT (Figure 3e) and IMP bound to F36L hHGPRT (Figure 5d) obtained using 260 nm excitation are compared with those obtained for the wild-type enzyme. The enzyme-induced perturbations in both IMP and GMP are analogous to those seen with the wild-type enzyme; the small differences are within experimental error (Tables 1 and 2). Thus, the active site environments of IMP and GMP in the wild-type and F36L hHGPRT enzymes are identical. This supports the conclusions made from kinetic

measurements of the forward reaction using hypoxanthine and guanine.[4]

**PfHGPRT and F36L hHGPRT Catalyze Xanthine and Bind to XMP, but the Active Site Pockets Are Dissimilar.** The UVRR spectrum of the 1:3 F36L hHGPRT/XMP solution shows specific shifts from the Raman spectrum of XMP at pH 7.0 (Figure 6e). The bands at 1573, 1531, 1469, 1391, and 1320 $cm^{-1}$ undergo downshifts of −2, −7, −11, −4, and −9 $cm^{-1}$, respectively (summarized in Table 3). The low signal-to-noise ratio in the observed spectrum is due to the low binding affinity of the enzyme for XMP.

The 2 $cm^{-1}$ downshift in the pyrimidine ring mode in the F36L hHGPRT·XMP complex is comparable to the 4 $cm^{-1}$ downshift observed in the PfHGPRT·XMP complex (refer to the previous discussion). The comparable magnitudes of the downshifts in the two cases suggest similar extents of reorganization of the pyrimidine ring in the active site pockets of the human and *Plasmodium* enzymes. A comparable downshift of −7 is observed in the C8−H bending and imidazole ring vibration (1531 $cm^{-1}$ mode in $XMP^-$), indicating strong interactions of this part of the nucleobase with the active site. Contrary to this, the N1−H bending vibrations undergoe downshifts of only 4 $cm^{-1}$ as opposed to average shifts of 10 and 7 $cm^{-1}$ in PfHGPRT (1391 $cm^{-1}$/1387 $cm^{-1}$ and 1337 $cm^{-1}$/1340 $cm^{-1}$ bands in anionic/neutral XMP). Thus, it appears that the exocyclic atoms of the pyrimidine ring make weaker contacts in F36L hHGPRT than in PfHGPRT.

Overall, more bands undergo large downshifts in the PfHGPRT·XMP complex than in the F36L hHGPRT·XMP complex, indicating that XMP makes more extensive contacts with PfHGPRT than with F36L hHGPRT.

**UVRR Spectra of the PfHGPRT·XMP Complex as a Function of pH.** To further investigate the change in the p$K_a$ of XMP upon binding to PfGHPRT, we conducted experiments with this complex at pH 8.5 and 6.5. At pH 8.5, we find that only the anionic form of XMP is bound because no bands corresponding to the neutral form are observed (Figure 6d). Further, we find that the intensity pattern and wavenumber shifts resemble those observed for the F36L hHGPRT·XMP complex. This implies that binding of anionic XMP to PfHGPRT at this pH occurs through interactions similar to those observed in the mutant human enzyme. The presence of the neutral form in the active site of PfHGPRT is then attributed to the unique ability of the malarial protein to modulate the p$K_a$. To confirm that the additional bands in the spectrum originate from the presence of a neutral species, we conducted experiments at pH 6.5. At this pH, the population in the protonated, neutral form should increase and the band corresponding to this species should undergo an increase in intensity. Indeed, we observed that the band at 1612 $cm^{-1}$ (neutral XMP) is intense compared to the band at 1568 $cm^{-1}$ (anionic XMP) (Figure 6b).

The ability of enzymes to perturb the ionization state of the bound ligand has been observed in other proteins. A mixture of neutral and anionic forms of uracil bound at the active site of uracil DNA glycosylase (UDG) was detected by NMR and normal Raman spectroscopy.[20] The p$K_a$ at the αC−H group of substrate analogue 3-thiaoctanoyl-CoA of medium-chain acyl-CoA dehydrogenase decreases when it binds to the enzyme.[23] The p$K_a$ shift of a cytosine in a viral ribozyme has been described previously by Carey and co-workers using Raman crystallography.[24] Nemeria et al. have shown the existence of different tautomers of thiamin diphosphate in four enzymes and the p$K_a$ of the 4′-aminopyrimidinium moiety varies among enzymes.[25]

## DISCUSSION

The high degree of similarity and the partially overlapping substrate specificity of hHGPRT and PfHGPRT provide an ideal set of enzymes to ask the fundamental question of how proteins discriminate between substrates and their analogues. HGPRT is a well-studied enzyme, and X-ray crystal structures of HGPRT in complex with the substrate analogues 7-hydroxy[4,3-*d*]pyrazolopyrimidine (HPP)[10] and 9-deazaguanine,[26] transition-state analogues immucillinGP[9] and immucillinHP,[13] and nucleotide products GMP,[12,27] IMP,[11,27] and XMP[28] are known. This rich structural information demonstrated that the human enzyme is highly flexible and undergoes a series of conformational changes as it moves along the catalytic cycle.[8] Molecular dynamics[29] simulations on the human and *Tritrichomonas fetus* HGPRTs have indicated that there is additional plasticity in the parasite analogues of HGPRT.[4,6] The next challenge is to understand how this plasticity of protein structure translates into differential chemical recognition of the substrates by the parasitic enzymes. This study provides a first step in the pursuit of these questions and shows through vibrational spectroscopy that subtle enzyme-induced distortion of the substrate is a part of the recognition strategy.

It is well established that HGPRT carries out catalysis via an ordered bi-bi mechanism.[11] Binding to the nucleotide is the first step in the backward reaction, after which $PP_i$ is bound. In this work, we have studied steady-state complexes of HGPRT bound to nucleotides IMP, GMP, and XMP. The use of resonance-enhanced Raman spectroscopy provides unprecedented selectivity for the vibrational signatures of the bound nucleotides over the protein environment.

At the outset, we find that H-bonding interactions seen in the crystal structures of hHGPRT·GMP[12] and hHGPRT·IMP[11] complexes are preserved in solution. UVRR data reported in this study show that the purine rings of IMP, GMP, and XMP are primarily anchored via hydrogen bonds observed in the reported crystal structures of human[11,12] and *Toxoplasma gondii*[27,28] HGPRTs.

Raman spectra of the HGPRT·substrate complexes also report on the nature of the active site interactions quantitatively. The bands of GMP undergo an overall downshift upon binding to the protein active site. This indicates a distortion of the structure of the GMP substrate to a more "anion-like" structure. This is also true of IMP and occurs in both enzymes. The large shifts in the C═O mode indicate its role in anchoring of the substrate to the active site. Nonresonant Raman spectra of G proteins, EF-Tu, and p21 with GDP and IDP[30] also demonstrated strong hydrogen bonding effects in the active site. The typical shifts in wavenumber for the ring vibrations were similar in magnitude to those observed in this study (∼7−10 $cm^{-1}$). The carbonyl stretching vibration was found to be perturbed by ∼20 $cm^{-1}$ in the p21·IDP complex. The fact that we observe a shift of 40 $cm^{-1}$ in the carbonyl mode in our data suggests that the HGPRT active site forms a stronger interaction with the purine C6═O group. Thus, Raman spectral shifts are sensitive to a range of interaction strengths between the enzyme and substrates, which in turn makes them more informative in conjunction with structures from other spectroscopies. These data

provide direct evidence of the distortion of the substrate by the enzyme. The magnitude and direction of perturbation of the vibrational Raman bands provide additional information about the nature of the distorted substrate.

The crystal structure of PfHGPRT bound to a product nucleotide is not available. Because the *Toxoplasma* and *Plasmodium* enzymes recognize xanthine, it is possible that their mode of recognition of IMP and GMP may be different from that of human HGPRT. Surprisingly, X-ray structures determined by Heroux et al.[27] revealed that the IMP and GMP complexes of TgHGPRT are similar to that of hHGPRT. Vibrational spectra of the PfHGPRT·product complexes observed in this work corroborate this conclusion. Similar Raman shifts of both human and *Plasmodium* product complexes suggest that despite differences in the overall protein structure, both enzymes ultimately assemble indistinguishable active site environments around IMP and GMP in solution. The observed similarity in the two active sites may be limited to the environment around the product, and additional differences may be present in the active sites assembled during the forward reaction of the enzyme.

Vibrational spectra add valuable information to known crystal structural data by identifying the protonation state of the bound ligand. Our experiments with the PfHGPRT·XMP complex have revealed the remarkable ability of this enzyme to alter the p$K_a$ of bound XMP. The TgHGPRT·XMP·$Mg^{2+}$ crystal structure shows that N3 of XMP is contacted by the $Mg^{2+}$ via a water molecule.[28] A similar interaction could be present in PfHGPRT as well, which leads to stabilization of XMP at the PfHGPRT active site. This structure can also be used to gain insight into the mechanism of xanthine recognition, which is exclusive to the protozoan HPRTs. The highly conserved aspartate residue adjacent to the C2═O group (Asp206 in TgHGPRT, Asp204 in PfHGPRT, and Asp193 in hHGPRT) is key in this mechanism. In the GMP structures, the backbone carbonyl of this residue forms hydrogen bonds with the exocyclic $NH_2$ group. In the TgHGPRT crystal structure with XMP,[27,28] this residue is rotated to minimize the repulsive interactions between the two carbonyl groups and, at the same time, to allow favorable H-bonding interactions with the backbone NH group (see Figure 2). This rotation is a result of shifting of the entire loop IV (residues 203−207 in TgHGPRT) of HGPRT. It has been hypothesized, on the basis of this structure and molecular dynamics simulations,[29] that human HGPRT lacks the required flexibility for shifting this loop, which is why it cannot use xanthine as a substrate. UVRR spectra demonstrate unequivocally that the mode of XMP binding is different in F36L hHGPRT and PfHGPRT. We find that PfHGPRT binds to both anionic and neutral XMP while mutant F36L hHGPRT can bind to only the anionic form. It is possible that the F36L mutation in hHGPRT allows a recovery of the flexibility of loop IV residues, such that xanthine can now be catalyzed. The fact that it still cannot bind to neutral XMP suggests that this recovery is only partial, resulting in a reaction $k_{cat}$ value that is far lower than that of PfHGPRT as observed. Thus, the data presented in this work provide evidence that further supports the current model of HGPRT action.

## ■ ASSOCIATED CONTENT

**Ⓢ Supporting Information.** UVRR ($\lambda_{exc}$ = 260 nm) spectra of the hHGPRT·AMP complex, hHGPRT alone, the hHGPRT·XMP complex, and the PfHGPRT·XMP complex in $D_2O$ and a table showing the effect of $\pi$ stacking on GMP. This material is available free of charge via the Internet at http://pubs.acs.org.

## ■ AUTHOR INFORMATION

### Corresponding Author

*National Centre for Biological Sciences, TIFR, GKVK Campus, Bellary Road, Bangalore 560065, India. Telephone: +91-80-23666160. Fax: +91-80-23636462. E-mail: puranik.mrinalini@gmail.com.

### Funding Sources

This work was supported by grants from the Department of Biotechnology, Government of India, to M.P. and H.B. and CSIR-NMITLI to H.B. M.P. is a recipient of the Innovative Young Biotechnologist Award, Department of Biotechnology, Government of India.

## ■ ABBREVIATIONS

HGPRT, hypoxanthine guanine phosphoribosyltransferase; UVRR, ultraviolet resonance Raman spectroscopy; GMP, guanosine monophosphate; IMP, inosine monophosphate; XMP, xanthosine monophosphate; PRPP, (*R*)-D-5-phosphoribosyl 1-pyrophosphate.

## ■ REFERENCES

(1) Ullman, B., and Carter, D. (1995) Hypoxanthine-guanine phosphoribosyltransferase as a therapeutic target in protozoal infections. *Infect. Agents Dis. 4*, 29–40.

(2) Senft, A. W., and Crabtree, G. W. (1983) Purine metabolism in the schistosomes: Potential targets for chemotherapy. *Pharmacol. Ther. 20*, 341–356.

(3) Dovey, H. F., Mckerrow, J. H., and Wang, C. C. (1984) Purine Salvage in *Schistosoma mansoni* Schistosomules. *Mol. Biochem. Parasitol. 11*, 157–167.

(4) Raman, J., Sumathy, K., Anand, R. P., and Balaram, H. (2004) A non-active site mutation in human hypoxanthine guanine phosphoribosyltransferase expands substrate specificity. *Arch. Biochem. Biophys. 427*, 116–122.

(5) Keough, D. T., Ng, A. L., Winzor, D. J., Emmerson, B. T., and de Jersey, J. (1999)Purification and characterization of *Plasmodium falciparum* hypoxanthine-guanine-xanthine phosphoribosyltransferase and comparison with the human enzyme. *Mol. Biochem. Parasitol. 98* 29–41.

(6) Keough, D. T., Skinner-Adams, T., Jones, M. K., Ng, A. L., Brereton, I. M., Guddat, L. W., and De Jersey, J. (2006) Lead compounds for antimalarial chemotherapy: Purine base analogs discriminate between human and *P. falciparum* 6-oxopurine phosphoribosyltransferases. *J. Med. Chem. 49*, 7479–7486.

(7) Subbayya, S. I. N., Sukumaran, S., Shivashankar, K., and Balaram, H. (2000) Unusual substrate specificity of a chimeric hypoxanthine-guanine phosphoribosyltransferase containing segments from the *Plasmodium falciparum* and human enzymes. *Biochem. Biophys. Res. Commun. 272*, 596–602.

(8) Keough, D. T., Brereton, I. M., De Jersey, J., and Guddat, L. W. (2005)The crystal structure of free human hypoxanthine-guanine phosphoribosyltransferase reveals extensive conformational plasticity throughout the catalytic cycle. *J. Mol. Biol. 351*, 170–181.

(9) Shi, W., Li, C. M., Tyler, P. C., Furneaux, R. H., Grubmeyer, C., Schramm, V. L., and Almo, S. C. (1999) The 2.0 Å structure of human hypoxanthine-guanine phosphoribosyltransferase in complex with a transition-state analog inhibitor. *Nat. Struct. Biol. 6*, 588–593.

(10) Balendiran, G. K., Molina, J. A., Xu, Y., Torres-Martinez, J., Stevens, R., Focia, P. J., Eakin, A. E., Sacchettini, J. C., and Craig, S. P., III (1999) Ternary complex structure of human HGPRTase, PRPP, $Mg^{2+}$,

and the inhibitor HPP reveals the involvement of the flexible loop in substrate binding. *Protein Sci. 8*, 1023–1031.

(11) Xu, Y., Eads, J., Sacchettini, J. C., and Grubmeyer, C. (1997) Kinetic mechanism of human hypoxanthine-guanine phosphoribosyltransferase: Rapid phosphoribosyl transfer chemistry. *Biochemistry 36*, 3700–3712.

(12) Eads, J. C., Scapin, G., Xu, Y., Grubmeyer, C., and Sacchettini, J. C. (1994) The crystal structure of human hypoxanthine-guanine phosphoribosyltransferase with bound GMP. *Cell 78*, 325–334.

(13) Shi, W., Li, C. M., Tyler, P. C., Furneaux, R. H., Cahill, S. M., Girvin, M. E., Grubmeyer, C., Schramm, V. L., and Almo, S. C. (1999) The 2.0 Å structure of malarial purine phosphoribosyltransferase in complex with a transition-state analogue inhibitor. *Biochemistry 38*, 9872–9880.

(14) Kulikowska, E., Kierdaszuk, B., and Shugar, D. (2004) Xanthine, xanthosine and its nucleotides: Solution structures of neutral and ionic forms, and relevance to substrate properties in various enzyme systems and metabolic pathways. *Acta Biochim. Pol. 51*, 493–531.

(15) Raman, J., Ashok, C. S., Subbayya, S. I. N., Anand, R. P., Selvi, S. T., and Balaram, H. (2005) *Plasmodium falciparum* hypoxanthine guanine phosphoribosyltransferase: Stability studies on the product-activated enzyme. *FEBS J. 272*, 1900–1911.

(16) Jayanth, N., Ramachandran, S., and Puranik, M. (2009) Solution Structure of the DNA Damage Lesion 8-Oxoguanosine from Ultraviolet Resonance Raman Spectroscopy. *J. Phys. Chem. A 113* 1459–1471.

(17) Gogia, S., Jain, A., and Puranik, M. (2009)Structures, Ionization Equilibria, and Tautomerism of 6-Oxopurines in Solution. *J. Phys. Chem. B 113*, 15101–15118.

(18) el Kouni, M. H. (2003) Potential chemotherapeutic targets in the purine metabolism of parasites. *Pharmacol. Ther. 99*, 283–309.

(19) Xu, Y., and Grubmeyer, C. (1998)Catalysis in human hypoxanthine-guanine phosphoribosyltransferase: Asp 137 acts as a general acid/base. *Biochemistry 37*, 4114–4124.

(20) Dong, J., Drohat, A. C., Stivers, J. T., Pankiewicz, K. W., and Carey, P. R. (2000)Raman Spectroscopy of Uracil DNA Glycosylase-DNA Complexes: Insights into DNA Damage Recognition and Catalysis. *Biochemistry 39*, 13241–13250.

(21) Unno, M., Kumauchi, M., Sasaki, J., Tokunaga, F., and Yamauchi, S. (2002)Resonance Raman Spectroscopy and Quantum Chemical Calculations Reveal Structural Changes in the Active Site of Photoactive Yellow. *Biochemistry 41*, 5668–5674.

(22) Thomas, A., and Field, M. J. (2006) A comparative QM/MM simulation study of the reaction mechanisms of human and *Plasmodium falciparum* HG(X)PRTases. *J. Am. Chem. Soc. 128*, 10096–10102.

(23) Nishina, Y., Sato, K., Tamaoki, H., Tanaka, T., Setoyama, C., Miura, R., and Shiga, K. (2003)Molecular Mechanism of the Drop in the pKa of a Substrate Analog Bound to Medium-Chain Acyl-CoA Dehydrogenase: Implications for Substrate Activation. *J. Biochem. 134*, 835–842.

(24) Gong, B., Chen, J.-H., Chase, E., Chadalavada, D. M., Yajima, R., Golden, B. L., Bevilacqua, P. C., and Carey, P. R. (2007) Direct Measurement of a pKa near Neutrality for the Catalytic Cytosine in the Genomic HDV Ribozyme Using Raman Crystallography. *J. Am. Chem. Soc. 129*, 13335–13342.

(25) Nemeria, N., Korotchkina, L., McLeish, M. J., Kenyon, G. L., Patel, M. S., and Jordan, F. (2007) Elucidation of the Chemistry of Enzyme-Bound Thiamin Diphosphate Prior to Substrate Binding: Defining Internal Equilibria among Tautomeric and Ionization States. *Biochemistry 46*, 10739–10744.

(26) Héroux, A., White, E. L., Ross, L. J., Kuzin, A. P., and Borhani, D. W. (2000)Substrate deformation in a hypoxanthine-guanine phosphoribosyltransferase ternary complex: The structural basis for catalysis. *Structure 8*, 1309–1318.

(27) Heroux, A., White, E. L., Ross, L. J., and Borhani, D. W. (1999) Crystal structures of the *Toxoplasma gondii* hypoxanthine-guanine phosphoribosyltransferase-GMP and -IMP complexes: Comparison of purine binding interactions with the XMP complex. *Biochemistry 38* 14485–14494.

(28) Heroux, A., White, E. L., Ross, L. J., Davis, R. L., and Borhani, D. W. (1999) Crystal structure of *Toxoplasma gondii* hypoxanthine-guanine phosphoribosyltransferase with XMP, pyrophosphate, and two $Mg^{2+}$ ions bound: Insights into the catalytic mechanism. *Biochemistry 38*, 14495–14506.

(29) Pitera, J. W., Munagala, N. R., Wang, C. C., and Kollman, P. A. (1999) Understanding substrate specificity in human and parasite phosphoribosyltransferases through calculation and experiment. *Biochemistry 38*, 10298–10306.

(30) Weng, G., Chen, C. X., Balogh-Nair, V., Callender, R., and Manor, D. (1994) Hydrogen bond interactions of G proteins with the guanine ring moiety of guanine nucleotides. *Protein Sci. 3*, 22–29.